STRUCTURAL BIOLOGY

Volume 79 (2023)

Supporting information for article:

X-ray structure of the metastable SEPT14–SEPT7 coiled coil reveals a hendecad region crucial for heterodimerization

Italo A. Cavini, Ashley J. Winter, Humberto D'Muniz Pereira, Derek N. Woolfson, Matthew P. Crump and Richard C. Garratt

Table S1 Macromolecule production information

Underlined sequences correspond to native septin residues. In some sequences, "GSHM" residues are the remains resulting from thrombin cleavage and cloning.

Source organism	*Homo sapiens*
DNA source	Reverse transcribed (SEPT6, SEPT7, SEPT8, SEPT10 and SEPT11) or synthetic (SEPT14)
Cloning/expression vector	pET28a (peptides), pOPINM (MBP fused), pETSUMO (SUMO fused)
Expression host	*E. coli* Rosetta(DE3) (peptides) or NEB T7 Express (fused constructs)
Amino-acid sequence of the peptide constructs (excluding the 17 residues tag cleaved by bovine thrombin)	>SEPT7C GSHMTYNGVDNNKNKGQLTKSPLAQMEEERREHVAKMKKMEMEMEQVFEM KVKEKVQKLKDSEAELQRRHEQMKKNLEAQHKELEEKRRQFEDEKANWEA QQRILEQQNSSRTLEKNKKKGKIF >SEPT7CCext GSHMAQMEEERREHVAKMKKMEMEMEQVFEMKVKEKVQKLKDSEAELQRR HEQMKKNLEAQHKELEEKRRQFEDEKANWEAQQRILEQ >SEPT7CC* (referred in previous publications as SEPT7CC) GSHMEMKVKEKVQKLKDSEAELQRRHEQMKKNLEAQHKELEEKRRQFEDE KANWEAQQRILEQ >SEPT14C GSHMWGFTDVGPNNQPVSFQEIFEAKRQEFYDQCQREEEELKQRFMQRVK EKEATFKEAEKELQDKFEHLKMIQQEEIRKLEEEKKQLEGEIIDFYKMKA ASEALQTQLSTDTKKDKHRKK >SEPT14CC* GSHMWQREEEELKQRFMQRVKEKEATFKEAEKELQDKFEHLKMIQQEEIR KLEEEKKQLEGEIIDFYKMKAASEA
Complete amino-acid sequence of the MBP- and SUMO-fused constructs (used in the SEC-SAXS experiments)	>SUMO-SEPT7c MGDSEVNQEAKPEVKPEVKPETHINLKVSDGSSEIFFKIKKTTPLRRLME AFAKRQGKEMDSLRFLYDGIRIQADQAPEDLDMEDNDIIEAHREQIGGSP LAQMEEERREHVAKMKKMEMEMEQVFEMKVKEKVQKLKDSEAELQRRHEQ MKKNLEAQHKELEEKRRQFEDEKANWEAQQRILEQQNSSRTLEKNKKKGK IFASLEHHHHHH >MBP-SEPT6c MAHHHHHHSSGMKIEEGKLVIWINGDKGYNGLAEVGKKFEKDTGIKVTVE HPDKLEEKFPQVAATGDGPDIIFWAHDRFGGYAQSGLLAEITPDKAFQDK LYPFTWDAVRYNGKLIAYPIAVEALSLIYNKDLLPNPPKTWEEIPALDKE LKAKGKSALMFNLQEPYFTWPLIAADGGYAFKYENGKYDIKDVGVDNAGA KAGLTFLVDLIKNKHMNADTDYSIAEAAFNKGETAMTINGPWAWSNIDTS KVNYGVTVLPTFKGQPSKPFVGVLSAGINAASPNKELAKEFLENYLLTDE GLEAVNKDKPLGAVALKSYEEELAKDPRIAATMENAQKGEIMPNIPQMSA FWYAVRTAVINAASGRQTVDEALKDAQTSGSPFSLQETYEAKRNEFLGEL QKKEEEMRQMFVQRVKEKEAELKEAEKELHEKFDRLKKLHQDEKKKLEDK KKSLDDEVNAFKQRKTAAELLQSQGSQAGGSQTLKRDKEKKN >MBP-SEPT8c MAHHHHHHSSGMKIEEGKLVIWINGDKGYNGLAEVGKKFEKDTGIKVTVE HPDKLEEKFPQVAATGDGPDIIFWAHDRFGGYAQSGLLAEITPDKAFQDK LYPFTWDAVRYNGKLIAYPIAVEALSLIYNKDLLPNPPKTWEEIPALDKE LKAKGKSALMFNLQEPYFTWPLIAADGGYAFKYENGKYDIKDVGVDNAGA KAGLTFLVDLIKNKHMNADTDYSIAEAAFNKGETAMTINGPWAWSNIDTS KVNYGVTVLPTFKGQPSKPFVGVLSAGINAASPNKELAKEFLENYLLTDE GLEAVNKDKPLGAVALKSYEEELAKDPRIAATMENAQKGEIMPNIPQMSA FWYAVRTAVINAASGRQTVDEALKDAQTSGSPFSLQETYEAKRKEFLSEL

QRKEEEMRQMFVNKVKETELELKEKERELHEKFEHLKRVHQEEKRKVEEK
RRELEEETNAFNRRKAAVEALQSQALHATSQQPLRKDKDKKN

> MBP-SEPT10c

MAHHHHHHSSGMKIEEGKLVIWINGDKGYNGLAEVGKKFEKDTGIKVTVE
HPDKLEEKFPQVAATGDGPDIIFWAHDRFGGYAQSGLLAEITPDKAFQDK
LYPFTWDAVRYNGKLIAYPIAVEALSLIYNKDLLPNPPKTWEEIPALDKE
LKAKGKSALMFNLQEPYFTWPLIAADGGYAFKYENGKYDIKDVGVDNAGA
KAGLTFLVDLIKNKHMNADTDYSIAEAAFNKGETAMTINGPWAWSNIDTS
KVNYGVTVLPTFKGQPSKPFVGVLSAGINAASPNKELAKEFLENYLLTDE
GLEAVNKDKPLGAVALKSYEEELAKDPRIAATMENAQKGEIMPNIPQMSA
FWYAVRTAVINAASGRQTVDEALKDAQTSGSPVSVQETYEAKRHEFHGER
QRKEEEMKQMFVQRVKEKEAILKEAERELQAKFEHLKRLHQEERMKLEEK
RRLLEEEIIAFSKKKATSEIFHSQSFLATGSNLRKDKDRKNSNFL

>MBP-SEPT11c

MAHHHHHHSSGMKIEEGKLVIWINGDKGYNGLAEVGKKFEKDTGIKVTVE
HPDKLEEKFPQVAATGDGPDIIFWAHDRFGGYAQSGLLAEITPDKAFQDK
LYPFTWDAVRYNGKLIAYPIAVEALSLIYNKDLLPNPPKTWEEIPALDKE
LKAKGKSALMFNLQEPYFTWPLIAADGGYAFKYENGKYDIKDVGVDNAGA
KAGLTFLVDLIKNKHMNADTDYSIAEAAFNKGETAMTINGPWAWSNIDTS
KVNYGVTVLPTFKGQPSKPFVGVLSAGINAASPNKELAKEFLENYLLTDE
GLEAVNKDKPLGAVALKSYEEELAKDPRIAATMENAQKGEIMPNIPQMSA
FWYAVRTAVINAASGRQTVDEALKDAQTSGSPFSLQETYEAKRNEFLGEL
QKKEEEMRQMFVMRVKEKEAELKEAEKELHEKFDLLKRTHQEEKKKVEDK
KKELEEEVNNFQKKKAAAQLLQSQAQQSGAQQTKKDKDKKNASFT

>MBP-SEPT14c

MAHHHHHHSSGMKIEEGKLVIWINGDKGYNGLAEVGKKFEKDTGIKVTVE
HPDKLEEKFPQVAATGDGPDIIFWAHDRFGGYAQSGLLAEITPDKAFQDK
LYPFTWDAVRYNGKLIAYPIAVEALSLIYNKDLLPNPPKTWEEIPALDKE
LKAKGKSALMFNLQEPYFTWPLIAADGGYAFKYENGKYDIKDVGVDNAGA
KAGLTFLVDLIKNKHMNADTDYSIAEAAFNKGETAMTINGPWAWSNIDTS
KVNYGVTVLPTFKGQPSKPFVGVLSAGINAASPNKELAKEFLENYLLTDE
GLEAVNKDKPLGAVALKSYEEELAKDPRIAATMENAQKGEIMPNIPQMSA
FWYAVRTAVINAASGRQTVDEALKDAQTSGSPVSFQEIFEAKRQEFYDQC
QREEEELKQRFMQRVKEKEATFKEAEKELQDKFEHLKMIQQEEIRKLEEE
KKQLEGEIIDFYKMKAASEALQTQLSTDTKKDKHRKK

Table S2 CC parameters and register assignment

Average values between chains are presented.

Residue from SEPT14	**Pos**	**φ (°)**	**φ-φ_0† (°)**	**Residue from SEPT7**	**Pos**	**φ (°)**	**φ-φ_0† (°)**	**Periodicity**	**$\Delta\varphi$ (°)**	**Core layer num.**	**Core-packing angle (°)**
Q346	*i*	**88.3**	-13.9	V347	*e*	**82.0**	10.4	3.63 (11/3)	6.3		
R347	*j*	**-169.9**	-9.1	A348	*f*	**178.3**	7.3	3.65 (11/3)	11.8		
E348	*k*	**-67.5**	-1.6	K349	*g*	**-82.2**	8.9	3.67 (11/3)	14.7		
E349	*a*	**30.4**	-3.6	M350	*h*	**14.3**	9.4	3.68 (11/3)	16.0	1	25.2 (parallel)
E350	*b*	**127.0**	-7.1	K351	*i*	**113.0**	10.8	3.68 (11/3)	14.0		
E351	*c*	**-131.8**	-6.0	K352	*j*	**-152.6**	8.2	3.68 (11/3)	20.8		
L352	*d*	**-36.6**	-8.3	M353	*k*	**-53.4**	12.5	3.69 (11/3)	16.8	2	64.7 (acute)
K353	*e*	**61.7**	-10.0	E354	*a*	**42.3**	8.3	3.69 (11/3)	19.4		
Q354	*f*	**159.5**	-11.5	M355	*b*	**139.5**	5.4	3.69 (11/3)	19.9		
R355	*g*	**-98.4**	-7.3	E356	*c*	**-126.2**	-0.4	3.70 (11/3)	27.8		
F356	*h*	**-3.9**	-8.8	M357	*d*	**-27.4**	0.8	3.71 (11/3)	23.5	3	71.7 (acute)
M357	*i*	**94.9**	-7.3	E358	*e*	**72.5**	0.9	3.70 (11/3)	22.4		
Q358	*j*	**-170.4**	-9.6	Q359	*f*	**170.2**	-0.8	3.69 (11/3)	19.4		
R359	*k*	**-71.7**	-5.8	V360	*g*	**-93.4**	-2.3	3.69 (11/3)	21.8		
V360	*a*	**25.9**	-8.1	F361	*h*	**3.3**	-1.7	3.70 (11/3)	22.6	4	15.4 (parallel)
K361	*b*	**124.0**	-10.1	E362	*i*	**100.2**	-2.0	3.69 (11/3)	23.8		
E362	*c*	**-141.1**	-15.3	M363	*j*	**-161.9**	-1.1	3.66 (11/3)	20.9		
K363	*d*	**-40.8**	-12.5	K364	*k*	**-60.3**	5.6	3.66 (11/3)	19.5	5	* (KTK)
E364	*e*	**57.5**	-14.2	V365	*a*	**36.2**	2.2	3.68 (11/3)	21.3		
A365	*f*	**157.9**	-13.1	K366	*b*	**137.3**	3.2	3.66 (11/3)	20.6		
T366	*g*	**-102.2**	-11.1	E367	*c*	**-124.8**	1.0	3.65 (11/3)	22.5		
F367	*h*	**-6.6**	-11.5	K368	*d*	**-28.9**	-0.6	3.66 (11/3)	22.3	6	72.6 (acute)
K368	*i*	**94.7**	-7.6	V369	*e*	**69.4**	-2.2	3.64 (11/3)	25.2		
E369	*j*	**-167.8**	-7.0	Q370	*f*	**167.4**	-3.6	3.65 (11/3)	24.8		
A370	*k*	**-67.9**	-2.0	K371	*g*	**-93.7**	-2.6	3.65 (11/3)	25.8		
E371	*a*	**32.6**	-1.4	L372	*h*	**3.9**	-1.0	3.65 (11/3)	28.6	7	24.0 (parallel)
K372	*b*	**133.4**	-0.7	K373	*i*	**103.4**	1.2	3.65 (11/3)	30.0		
E373	*c*	**-128.2**	-2.4	D374	*j*	**-158.3**	2.5	3.63 (11/3)	30.1		
L374	*d*	**-28.6**	-0.3	S375	*k*	**-58.7**	7.2	3.64 (11/3)	30.1	8	51.9 (acute)
Q375	*e*	**69.1**	-2.6	E376	*a*	**37.6**	3.6	3.65 (11/3)	31.5		
D376	*f*	**166.7**	-4.3	A377	*b*	**136.6**	2.5	3.63 (11/3)	30.1		
K377	*g*	**-93.7**	-2.6	E378	*c*	**-124.9**	0.9	3.63 (11/3)	31.2		
F378	*h*	**-2.5**	-7.5	L379	*d*	**-28.7**	-0.5	3.62 (11/3)	26.2	9	80.6 (acute)
E379	*i*	**101.1**	-1.1	Q380	*e*	**71.8**	0.1	3.59 (11/3)	29.4		
H380	*j*	**-157.5**	3.3	R381	*f*	**172.6**	1.6	3.60 (11/3)	29.8		
L381	*k*	**-57.9**	8.0	R382	*g*	**-88.4**	2.8	3.58 (11/3)	30.4		
K382	*a*	**44.1**	10.2	H383	*h*	**11.9**	7.0	3.55 (11/3)	32.2	10	* (KTK)
M383	*b*	**146.6**	12.5	E384	*i*	**113.8**	11.6	3.54 (11/3)	32.8		
I384	*c*	**-111.6**	14.2	Q385	*j*	**-145.2**	15.6	3.55 (11/3)	33.6		
Q385	*d*	**-12.6**	15.7	M386	*k*	**-45.2**	20.7	3.55 (11/3)	32.7	11	72.4 (acute)
Q386	*e*	**92.4**	21.5	K387	*e*	**60.1**	-11.6	3.52 (7/2)	32.3		

E387	*f*	**-164.4**	21.8	K388	*f*	**160.8**	-10.2	3.52 (7/2)	34.8		
E388	*g*	**-60.3**	23.0	N389	*g*	**-98.4**	-7.3	3.55 (7/2)	38.1		
I389	*a*	**42.5**	23.0	L390	*h*	**1.8**	-3.1	3.57 (7/2)	40.7	12	44.5 (acute)
R390	*b*	**141.9**	19.5	E391	*i*	**106.3**	4.1	3.56 (7/2)	35.6		
K391	*c*	**-116.8**	18.0	A392	*j*	**-153.3**	7.5	3.55 (7/2)	36.5		
L392	*d*	**-14.3**	17.6	Q393	*k*	**-51.7**	14.2	3.55 (7/2)	37.4	13	59.4 (acute)
E393	*e*	**86.9**	16.0	H394	*a*	**49.3**	29.8	3.55 (7/2)	37.6		
E394	*f*	**-171.1**	15.2	K395	*b*	**150.4**	28.1	3.55 (7/2)	38.5		
E395	*g*	**-69.4**	13.9	E396	*c*	**-108.3**	26.4	3.55 (7/2)	38.9		
K396	*a*	**32.5**	13.0	L397	*d*	**-8.8**	23.1	3.55 (7/2)	41.3	14	42.8 (acute)
K397	*b*	**134.3**	12.0	E398	*e*	**94.0**	23.0	3.54 (7/2)	40.4		
Q398	*c*	**-123.7**	11.1	E399	*f*	**-165.0**	21.2	3.56 (7/2)	41.3		
L399	*d*	**-22.5**	9.4	K400	*g*	**-64.5**	18.9	3.55 (7/2)	42.0	15	59.6 (acute)
E400	*e*	**82.5**	11.6	R401	*a*	**36.5**	17.0	3.53 (7/2)	46.0		
G401	*f*	**-176.1**	10.1	R402	*b*	**138.1**	15.8	3.53 (7/2)	45.8		
E402	*g*	**-74.0**	9.4	Q403	*c*	**-120.9**	13.8	3.52 (7/2)	47.0		
I403	*a*	**29.7**	10.2	F404	*d*	**-20.2**	11.7	3.53 (7/2)	49.9	16	52.8 (acute)
I404	*b*	**133.9**	11.6	E405	*e*	**80.9**	10.0	3.53 (7/2)	53.0		
D405	*c*	**-125.4**	9.4	D406	*f*	**-177.6**	8.6	3.53 (7/2)	52.2		
F406	*d*	**-26.3**	5.6	E407	*g*	**-76.7**	6.7	3.52 (7/2)	50.3	17	53.8 (acute)
Y407	*e*	**72.2**	1.3	K408	*a*	**25.0**	5.5	3.51 (7/2)	47.2		
K408	*f*	**176.3**	2.6	A409	*b*	**126.9**	4.6	3.53 (7/2)	49.4		
M409	*g*	**-81.3**	2.0	N410	*c*	**-130.7**	4.1	3.54 (7/2)	49.4		
K410	*a*	**21.0**	1.5	W411	*d*	**-30.0**	1.9	3.55 (7/2)	51.0	18	50.6 (acute)
A411	*b*	**119.8**	-2.6	E412	*e*	**70.6**	-0.3	3.56 (7/2)	49.2		
A412	*c*	**-140.3**	-5.5	A413	*f*	**171.3**	1.8	3.58 (7/2)	48.4		
S413	*d*	**-40.4**	-8.4	Q414	*g*	**-87.0**	-3.6	3.59 (7/2)	46.6		

[†] φ_0 denotes Crick angles used for comparison. Two different sets of φ_0 were used for hendecads and heptads, respectively (see Methods).

[*] In these layers, no KIH interaction was found by Socket2.

Table S3 SEC-SAXS data and analysis.

SASBDB entry	**SASDR39**	**SASDR49**	**SASDR59**	**SASDR69**	**SASDR79**
Sample	**MBP-6c+ SUMO-7c**	**MBP-8c+ SUMO-7c**	**MBP-10c+ SUMO-7c**	**MBP-11c+ SUMO-7c**	**MBP-14c+ SUMO-7c**
Instrumental					
Instrument and SEC parameters	B21 Diamond Light Source; Superdex 200 Increase 3.2/300; 0.075 ml/min; injection concentration, 5.0 mg/ml; injection volume, 45 µl				
Buffer	50 mM Tris-HCl, 150 mM NaCl, pH 7.5				
Buffer/sample additives	none	none	none	none	1 mM DTT
Elution volume (ml)	1.328	1.327	1.312	1.314	1.332
Guinier analysis					
$I(0)$ (cm^{-1}) (± 0.0002)	0.0847	0.0712	0.0931	0.0612	0.0635
Reciprocal space R_g (Å)	54.4 ± 0.2	52.7 ± 0.2	56.6 ± 0.3	52.4 ± 0.3	51.0 ± 0.2
q_{min} (calculated q_{min} max, π/D_{max}) ($Å^{-1}$)	0.0092 (0.0146)	0.0104 (0.0158)	0.0110 (0.0145)	0.0096 (0.0150)	0.0129 (0.0155)
$q.R_g$ max	1.175	1.199	1.119	1.167	1.162
r^2	0.991	0.994	0.992	0.991	0.994
***P*(*r*) analysis**					
$I(0)$ (cm^{-1}) (± 0.0002)	0.0892	0.0723	0.0946	0.0627	0.0653
Real space R_g (Å)	59.2 ± 0.2	56.6 ± 0.2	60.4 ± 0.2	57.3 ± 0.2	56.0 ± 0.2
D_{max} (Å)	215	199	217	209	203
q range, also used for model fitting and atomistic modelling ($Å^{-1}$)	0.0092-0.2329	0.0104-0.2055	0.0110-0.2197	0.0096-0.2236	0.0129-0.2355
χ^2 (total estimate from GNOM)	1.454 (0.50)	1.574 (0.56)	1.866 (0.63)	1.324 (0.64)	1.465 (0.66)
Porod volume, V_p (10^3 $Å^{-3}$)	269	264	298	258	259
Ratio V_p/calculated M	3.4	3.3	3.7	3.2	3.2
Resolution (from SASRES) (Å)	36.24	41.53	38.42	38.51	42.19
DATCLASS shape	extended	extended	extended	extended	extended
Molecular mass determination (ratio to expected value)					
Expected heterodimeric MW from sequences (Da)	80,196	80,622	80,844	80,604	80,018
MW from Bayesian inference (kDa)	85.7 (1.07)	88.3 (1.10)	94.2 (1.17)	85.7 (1.06)	88.3 (1.10)
MW from SAXSMoW (kDa)	92.4 (1.15)	91.1 (1.13)	101.2 (1.25)	86.4 (1.07)	92.8 (1.16)
MW from V_c (kDa)	71.8 (0.90)	73.8 (0.92)	80.0 (0.99)	70.1 (0.87)	76.1 (0.95)
Shape model fitting					
Symmetry, anisotropy assumptions	P1, none	P1, none	P1, none	P1, none	P1, none
DAMMIF (fast, default parameters, 23 reconstructions):					
NSD (standard deviation)	0.78 (0.08)	0.72 (0.14)	0.79 (0.07)	0.82 (0.08)	0.68 (0.07)
DAMMIN (expert mode, $r_{dummy\ atoms}$ = 5 Å):					
χ^2	1.468	1.582	1.869	1.321	1.479
Atomistic modelling					
MultiFoXS (unique state, flexible linkers†, 10,000 iterations):					
Model	hetP: hetero-parallel, AlphaFold-multimer model				
R_g (Å)	56.61	54.40	54.23	54.92	52.83
χ^2	1.61	1.61	2.71	1.29	1.54
c_1, c_2	1.00, 0.94	0.99, 1.21	0.99, 1.98	1.00, 0.49	0.99, 2.07
Model	hetAP: hetero-antiparallel, CCbuilder model				
R_g (Å)	52.82	53.57	53.63	54.60	52.02
χ^2	4.54	4.73	4.30	3.09	5.54
c_1, c_2	0.99, 2.07	1.00, 4.00	0.99, 3.01	0.99, 2.56	0.99, 3.64
FoXS (ensemble):					
Model	hetP*: hetero-parallel MultiFoXS solution + MBP-fused homo-antiparallel based on the coiled-coil structure of SEPT8C				
R_g (Å)	54.23, 84.97				
weight (%)	94.3, 5.7				
χ^2	2.42				
c_1, c_2	1.00, 2.00				

†Tripeptide linker plus adjacent residues: 378-382 aa (in MBP-fused proteins), 96-100 aa (in SUMO-7c).

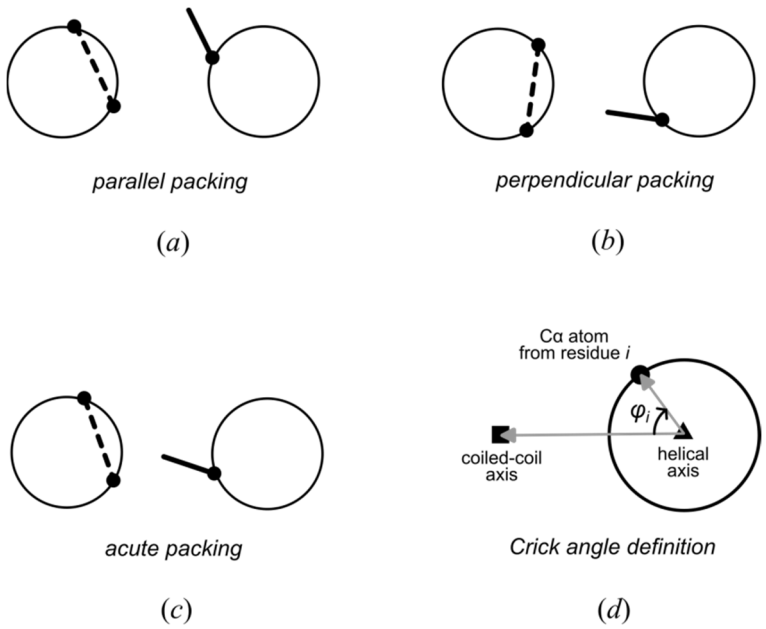

Figure S1 Packing geometries and Crick angle definition in CCs. (*a*) Parallel, (*b*) perpendicular and (*c*) acute packing. The former two are generally seen in *a*-*a* and *d*-*d* core layers in parallel dimers; the latter is present in three-helical bundles. The terms parallel and perpendicular arise from the relationship between the Cα-Cβ vector of the side-chain knob from one helix (solid line) and the Cα-Cα vector of the consecutive residues which form the floor of the corresponding hole in the adjacent helix (dashed lines). Acute packing angles are only possible in dimers if an asymmetry exists (*i.e.*, rotation in one of the helices). Thick and dashed lines represent the direction of the Cα-Cβ vector of the knob and the base of the hole, respectively. Circumferences represent the backbone of the α-helices. (*d*) Definition of the Crick angle (φ_i), *i.e.*, the angle between the vector connecting the centre of the helix (triangle) to the superhelical axis (square) and the vector between the former and the Cα of a given residue *i* of the helix (circle).

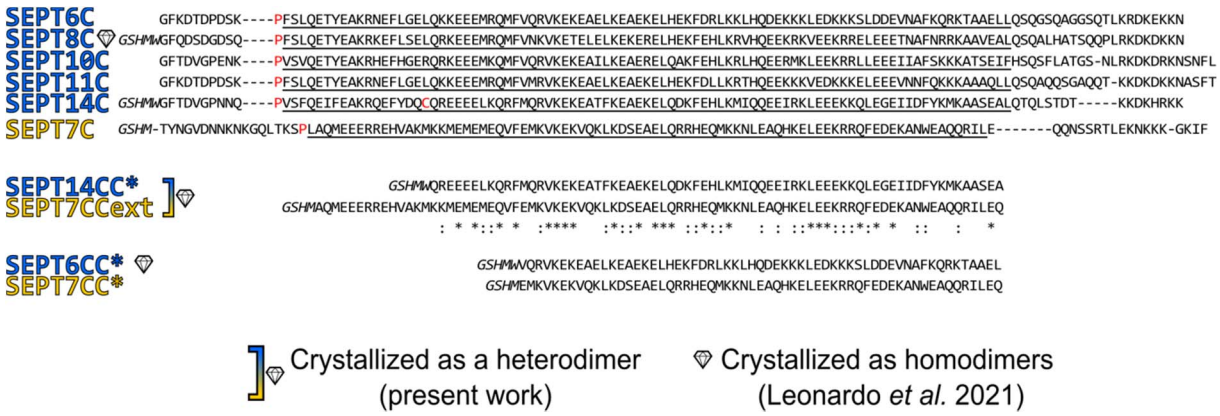

Figure S2 Sequence alignment of septin *C*-terminal domains and CC constructs used in the present work or elsewhere. The putative CC region is underlined in the full CTDs sequences. Non-native residues are shown in italics. The proline residues which likely interrupt the CC and C345 from

SEPT14 are highlighted in red. SEPT14CC* and SEPT7CCext, the constructs crystallized here as heterodimers, have 31% (small asterisks) and 59% (asterisks plus double dots) sequence identity and similarity, respectively.

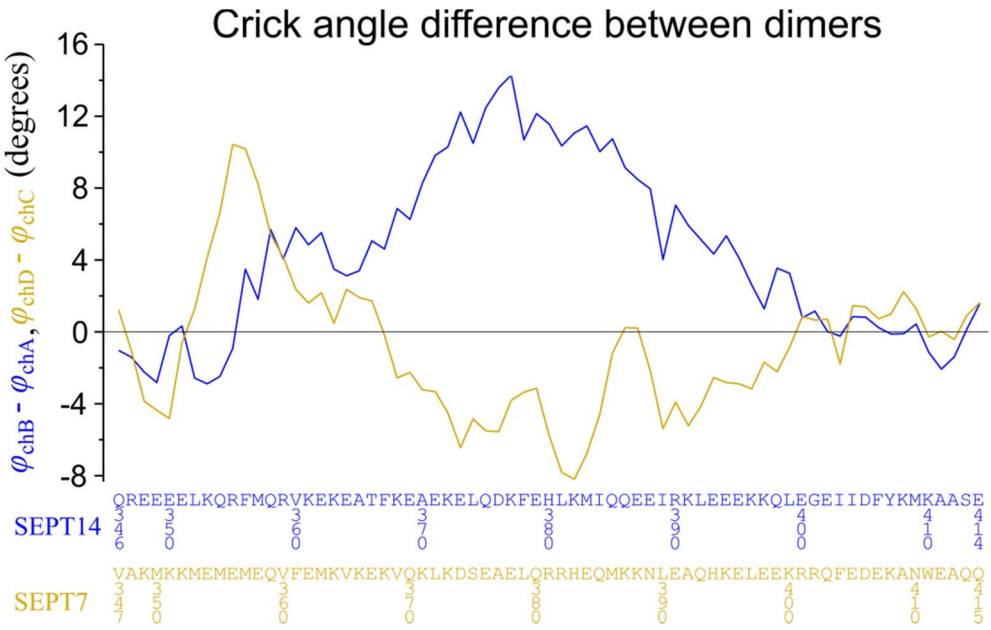

Figure S3 Crick angle differences between residues in chains A and B (SEPT14, blue) and in chains C and D (SEPT7, yellow). Heterodimers are formed by chains AC and BD.

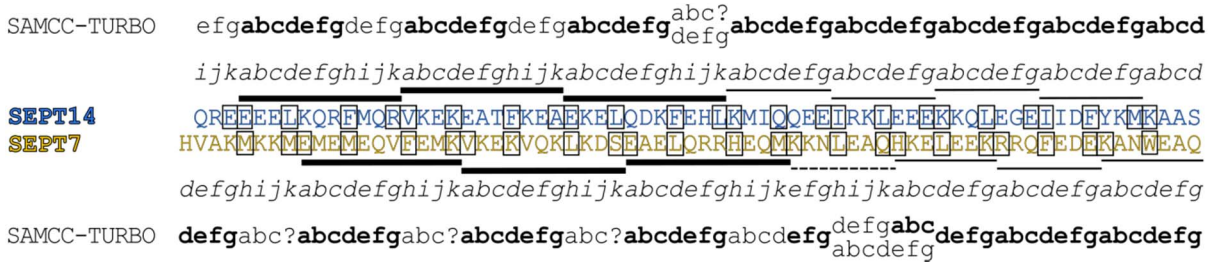

Figure S4 Register output by SamCC-Turbo. Italic, register adopted; bold, register in agreement to the adopted. SamCC-Turbo identifies correctly the hendecads in the structure (thick lines), by adding "*abc?*" or "*defg*" to a heptad. In the heptads at the *C* terminus (fine lines), SamCC-Turbo recognizes mixed *d-ag* core layers. Due to differences in dimers AC and BD, assignments are ambiguous in certain regions. The first heptad in SEPT7 (dashed line) is better assigned as *efghijk* (instead of *abcdefg*).

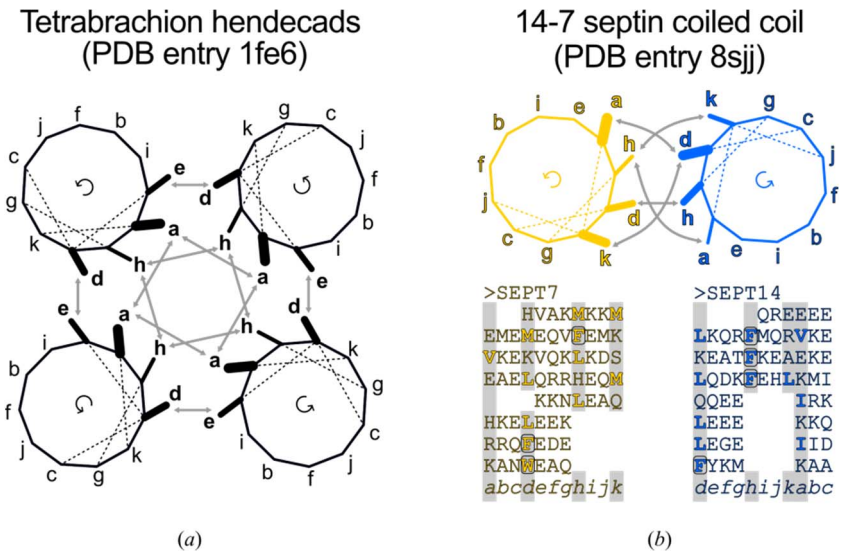

Figure S5 CC packing layers of hendecads in (*a*) the tetrameric tetrabrachion (PDB entry 1fe6) and (*b*) in the present heterodimeric structure (PDB entry 8sjj). Core layers are indicated (grey arrows). A repeat scheme for the present structure is shown; grey, core residues; bold, hydrophobic residues; rectangles, aromatic hydrophobic residues.

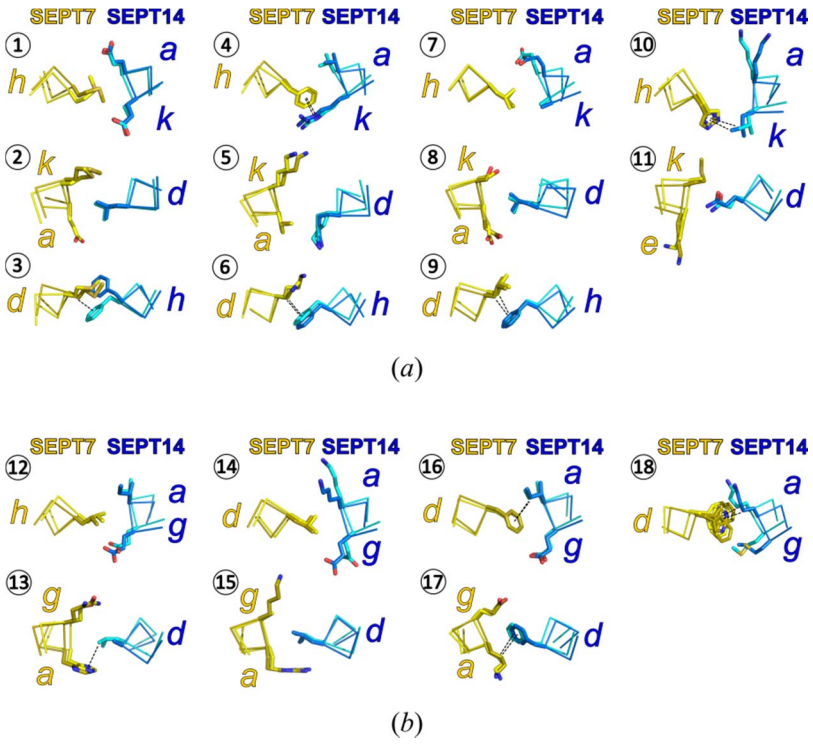

Figure S6 Core layers in (*a*) hendecads and in (*b*) heptads of the SEPT14-SEPT7 CC structure (PDB entry 8sjj). Both dimers are represented (A-C, cyan-yellow; B-D, blue-gold). Numbers represent the core number, from *N* to *C* termini. π interactions involving aromatic residues are indicated (dashed lines). Superposition is only local and do not reflect the superposition of the whole structure.

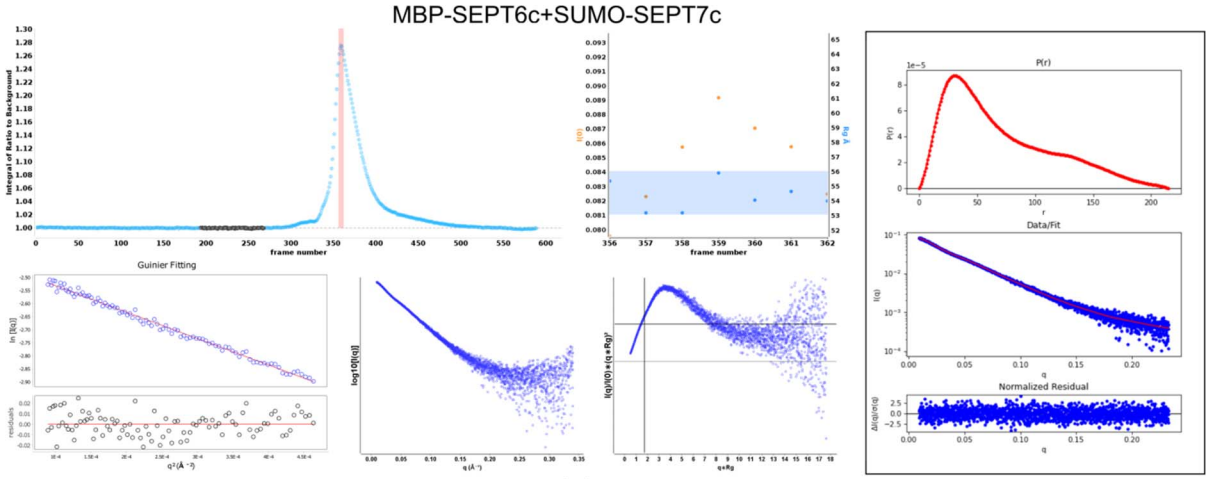

(*a*)

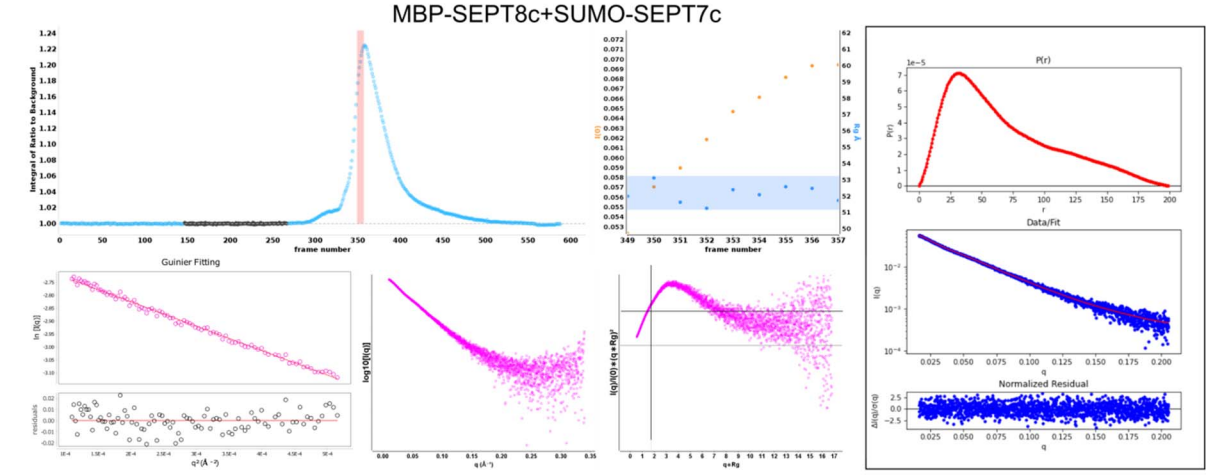

(*b*)

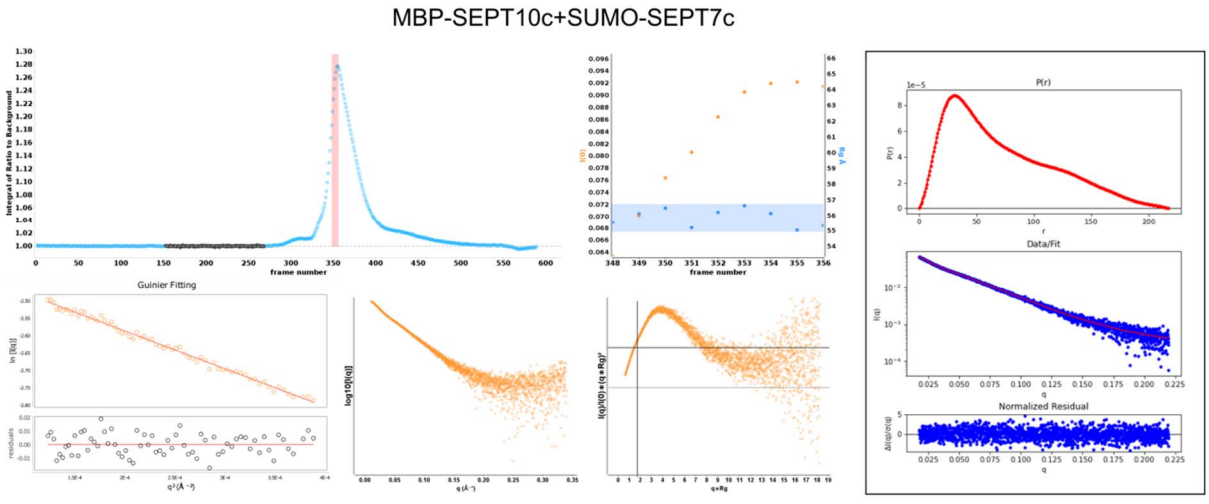

(*c*)

(continue next page)

(continuation of **Fig. S7**)

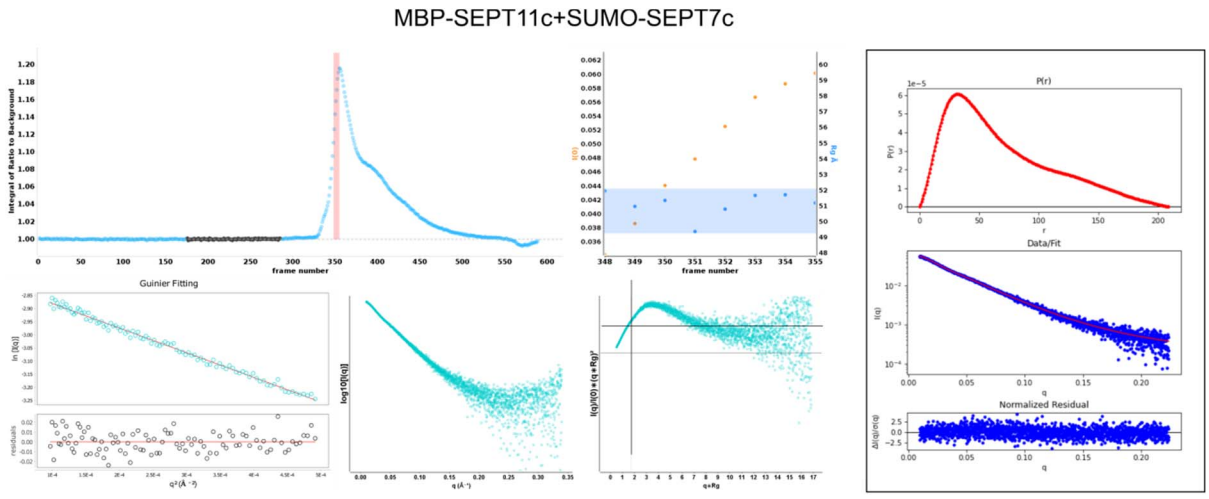

(*d*)

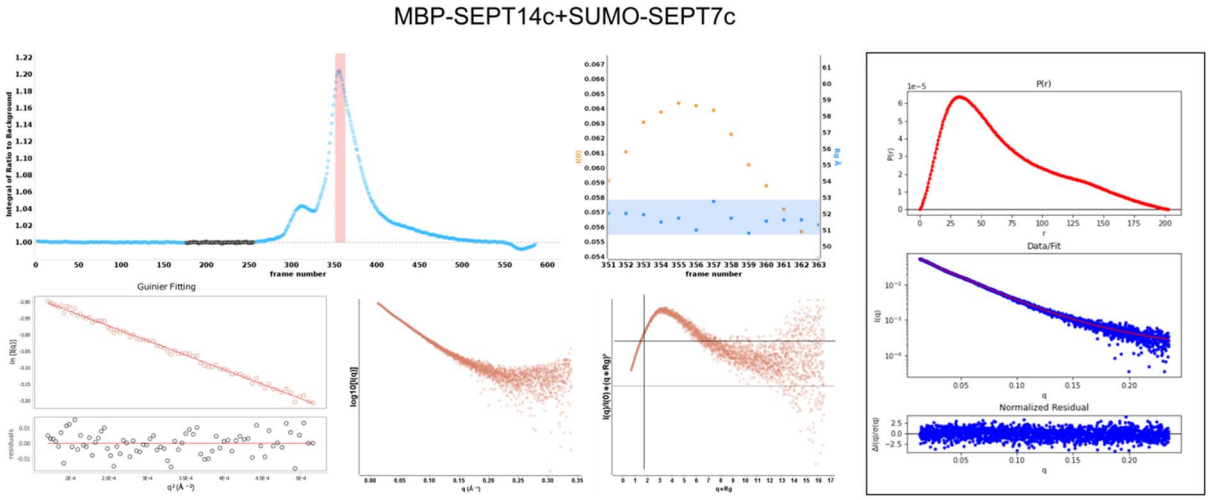

(*e*)

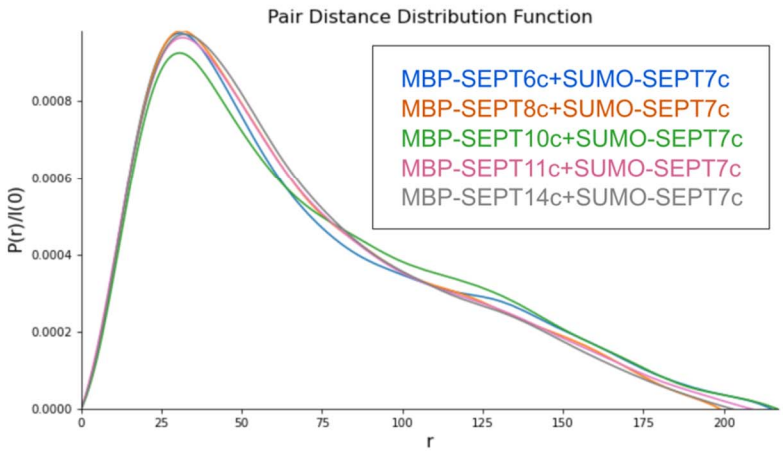

(*f*)

Figure S7 SEC-SAXS data collection parameters and statistics. Samples consisted of SUMO-SEPT7c mixed in equimolar proportions with (*a*) MBP-SEPT6c, (*b*) MBP-SEPT8c, (*c*) MBP-

SEPT10c, (*d*) MBP-SEPT11c and (*e*) MBP-SEPT14c. Top row (from left to right): SEC profile (cyan dots) showing regions used for buffer subtraction (black dots) and data treatment (coral region); $I(0)$ (orange) and R_g (blue) across the selected frames. Bottom row (from left to right): Guinier fit and residuals for data at $q*R_g < 1.3$; $I(q)$ versus q semi-log plot; dimensionless Kratky plot with crosshair (1.10, 1.73) indicating the expected peak maxima for a globular, folded protein. Insert at the right: pair-distance, $P(r)$ distribution (top) with the fit of the $P(r)$ profile in red to the raw scattering data in blue (middle) and the normalized residuals (bottom). (*f*) Superposition of the $P(r)$ functions ($I(0)$, cm^{-1} *vs* r, Å).

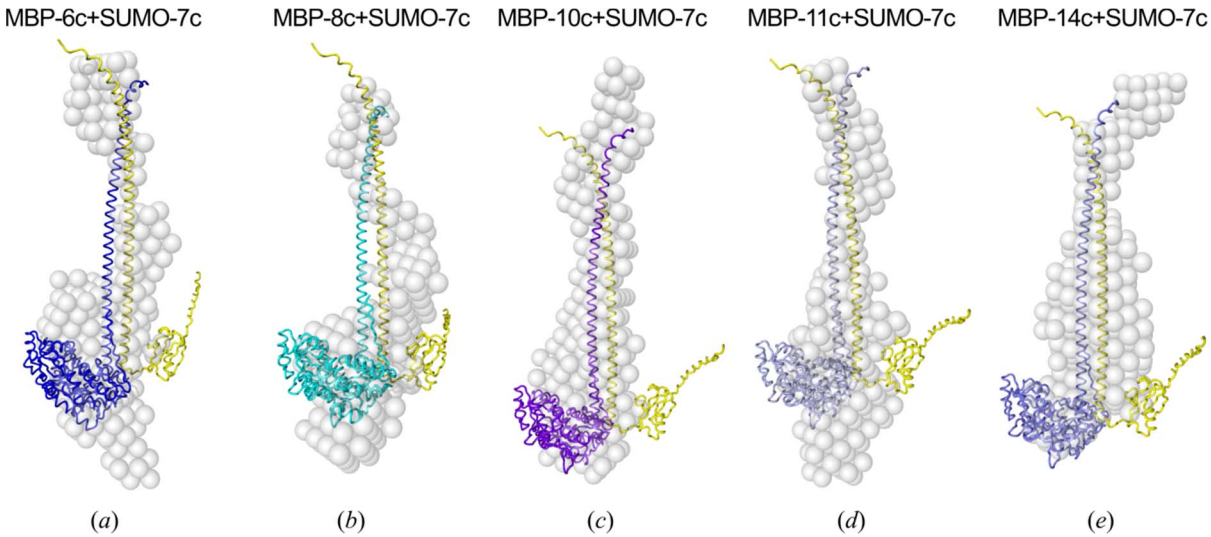

Figure S8 Bead density fitting of the SEC-SAXS data using *ab initio* DAMMIN dummy atom models. The AlphaFold-multimer hetero-parallel predicted models were superimposed onto the bead models using CIFSUP.

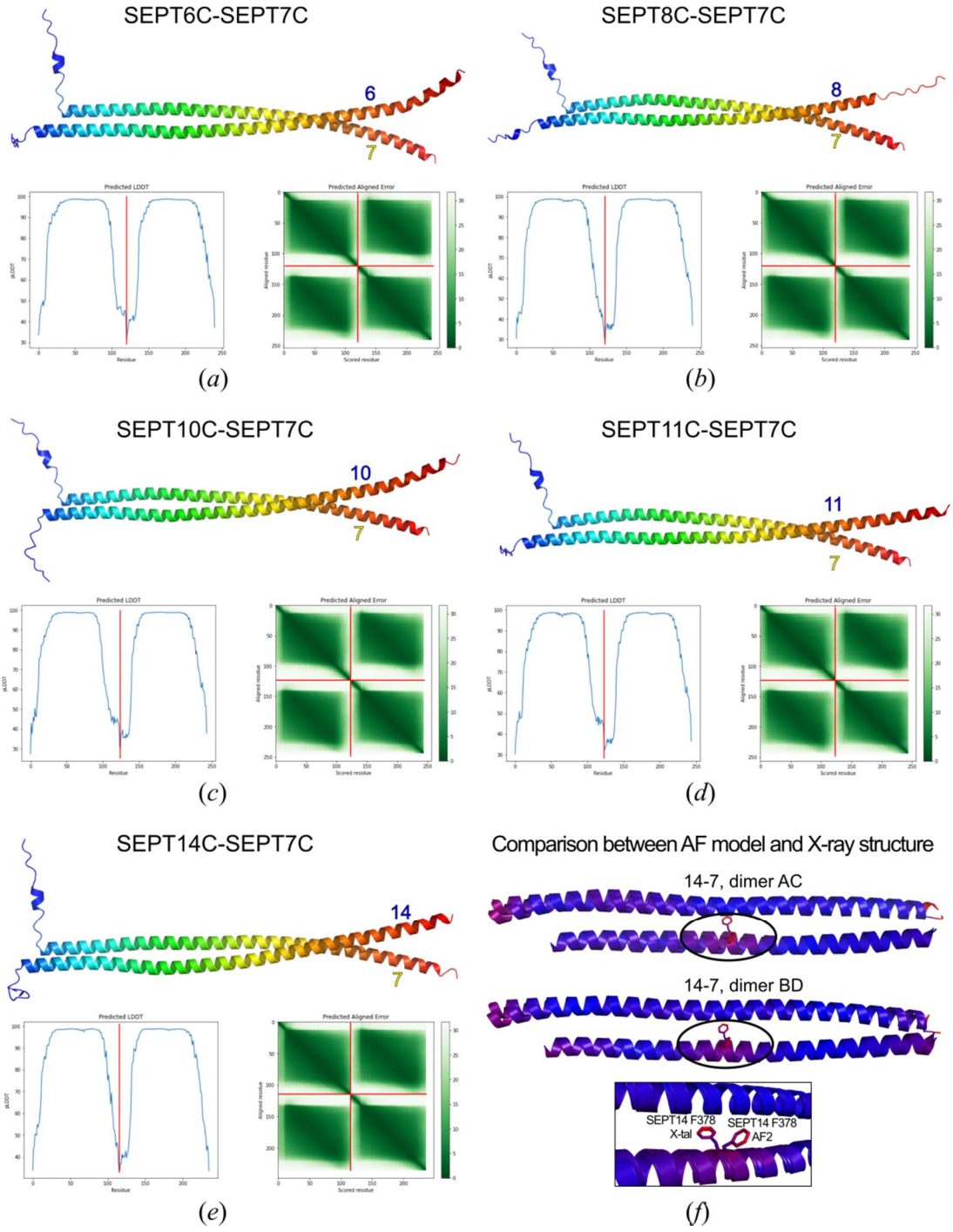

Figure S9 AlphaFold-multimer models for (*a*) SEPT6C-SEPT7C, (*b*) SEPT8C-SEPT7C, (*c*) SEPT10C-SEPT7C, (*d*) SEPT11C-SEPT7C and (*e*) SEPT14C-SEPT7C septin CC heterodimers. Chains are coloured from *N* to *C* termini, blue to red. The confidence metrics pLDDT and PAE are plotted. The average pLDDT is 90.1, 89.7, 89.2, 88.9, 90.7 for 6C-7C, 8C-7C, 10C-7C, 11C-7C and 14C-7C, respectively. (*f*) Comparison between crystallographic dimers AC and BD and the AlphaFold-multimer model (RMSDs of 1.45 and 1.61 Å, respectively). Atoms are coloured from low (blue) to high RMSD (red). The inset shows the different conformation of Phe378 from SEPT14 between the predicted and the crystallographic model (RMSD of 9.2 Å).

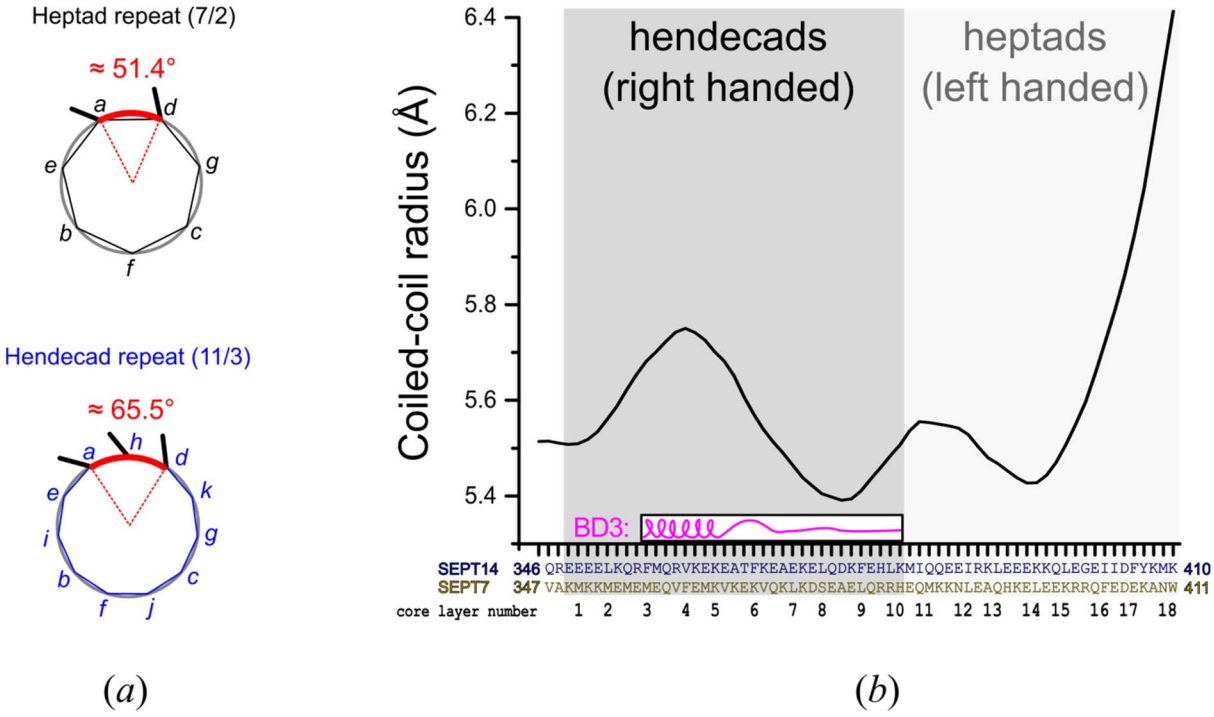

Figure S10 Presence of hendecad repeats in the septin heterodimeric CC is important for the binding of partners. (*a*) Core positions in hendecads are distributed at a wider angle than in heptads, broadening the interface. (*b*) CC radius averaged over a seven-residue window and also between AC and BD dimers. The binding site of BD3 from Borg's (magenta) is indicated (Castro *et al.* 2023). The binding of the helical region of BD3 corresponds to the widest point of the hendecad region of the structure.